Fully symmetric and doubly degenerate coherent phonons in semimetals at low temperature and high excitation: similarities and differences

2006 J. Phys.: Condens. Matter 18 10571

(http://iopscience.iop.org/0953-8984/18/47/005)

INSTITUTE OF PHYSICS PUBLISHING JOURNAL OF PHYSICS: CONDENSED MATTER

J. Phys.: Condens. Matter **18** (2006) 10571–10584 doi:10.1088/0953-8984/18/47/005

Fully symmetric and doubly degenerate coherent phonons in semimetals at low temperature and high excitation: similarities and differences

O V Misochko[1], K Ishioka[2], Muneaki Hase[3] and M Kitajima[2]

[1] Institute of Solid State Physics, Russian Academy of Sciences, 142432 Chernogolovka, Moscow region, Russia
[2] National Institute for Materials Science, 1-2-1 Sengen, Tsukuba 305-0047, Ibaraki, Japan
[3] Institute of Applied Physics, University of Tsukuba, 1-1-1 Tennodai, Tsukuba 305-8573, Japan

E-mail: misochko@issp.ac.ru

Received 18 September 2006, in final form 23 October 2006
Published 8 November 2006
Online at stacks.iop.org/JPhysCM/18/10571

Abstract

We report the ultrafast dynamics of simultaneously excited coherent A_{1g} and E_g phonons in semimetals Bi and Sb. At a low level of excitation, the doubly degenerate E_g phonons in pump–probe data occur at low temperature only, and they nearly vanish at room temperature. Their initial phase is shifted by $\pi/2$ with respect to that of the fully symmetric A_{1g} phonons indicating that the E_g and A_{1g} phonons are excited predominantly impulsively and displacively, respectively. At a high level of excitation, both phonons display an asymmetric (varying in time) line shape with more spectral weight at low frequencies testifying to quantum interference between the one-phonon state and a continuum of states. Furthermore, above a threshold fluence, these phonons of different symmetry exhibit collapse and revival, albeit with different characteristic times.

1. Introduction

There have been extensive experimental studies of the ultrafast dynamics of crystal lattices, making use of the coherence of phonons [1, 2]. The common feature in all these experiments is the generation of superpositions of lattice states that evolve in time coherently (when more than two energy levels are involved, the possibility of interference arises). The necessary requirement for coherent phonon excitation is the availability of Raman active phonons with frequency smaller than the inverse of the pulse duration. For low fluence excitation, when the oscillation amplitude is linear in the fluence, the vibrational properties such as the spectrum and decay of coherent phonons are considered as intrinsic properties of the crystal. Such a simple and relatively well understood picture changes radically as one enters the non-linear regime [3–12], where the intense laser pulses produce a high density of phonons and free

carriers thereby modifying the phonon–phonon and electron–phonon coupling. To date, the high fluence excitation has been used to drive only fully symmetric phonons, whose generation mechanism had been identified as a transient stimulated Raman scattering in the displacive limit [1].

A number of publications deal with the time-domain spectroscopy of semimetals, having large amplitude, low frequency coherent oscillations [4–8, 10–18]. Below we only summarize the main ideas and results relevant to our study. The semimetals bismuth and antimony both crystallize in the rhombohedral (A7) structure with two atoms in the unit cell. Consequently, the crystals have two Raman active phonons of symmetries A_{1g} (fully symmetric, diagonal) and E_g (doubly degenerate) with the corresponding second-rank tensors

$$A_{1g} = \begin{pmatrix} a & & \\ & a & \\ & & b \end{pmatrix} \qquad \text{and} \qquad E_g = \begin{pmatrix} d & & \\ & -d & f \\ & f & \end{pmatrix}, \qquad \text{or} \qquad E_g = \begin{pmatrix} & -d & -f \\ -d & & \\ -f & & \end{pmatrix}. \tag{1}$$

Their frequencies at room temperature determined by spontaneous Raman scattering are ≈2.9 and ≈2.2 THz for bismuth, and ≈4.5 and ≈3.5 THz for antimony [19, 20]. Early femtosecond pump–probe experiments carried out with isotropic detection at room temperature revealed only coherent oscillations corresponding to fully symmetric modes [13, 14]. Since then, the mechanisms responsible for the generation of coherent phonons in absorbing materials have been extensively discussed, especially in recent years [1, 2, 17, 18]. The absence of non-fully symmetric phonons in the early experiments [13, 14] motivated the development of a model called displacive excitation of coherent phonons (DECP). In the DECP model [15], the equilibrium positions of the atoms experience an abrupt shift due to coupling with excited carriers created by the ultrashort laser pulse. This model, accounting reasonably well for the available experimental results, provided a straightforward explanation for driving fully symmetric modes, and seemed to be unrelated to Raman scattering. However, the modifications of detection schemes, such as a polarization analysis of the reflected light, revealed the simultaneous excitation of non-fully symmetric modes in Bi [16] and Sb [18], as well as in Te [21]. A later theoretical consideration rendered the DECP model a particular case of resonant Raman scattering in that the driving force can contain both impulsive and displacive components [1, 18].

Recently, it was demonstrated that, under intense optical excitation, the frequency of the fully symmetric phonon in Bi depends on the time delay on a picosecond timescale. That is, the phonon has a positive chirp arising either from lattice anharmonicity [5, 6], or from time dependence of the electron–hole plasma density [11]. At the same time, it was suggested that the doubly degenerate phonons in Bi can contribute to the coherent lattice dynamics studied even with isotropic detection [5]. Later it was shown that at a greater fluence exceeding a well-defined threshold, the amplitude of the fully symmetric oscillation exhibits a collapse and revival with characteristic times strongly dependent on the duration and fluence of the pump pulse [6, 8, 10].

In our paper we provide spectroscopic evidence for a *simultaneous* excitation of the fully symmetric A_{1g} and doubly degenerate E_g phonons in bismuth and antimony at low temperature and high excitation. Additionally, we demonstrate that the A_{1g} and E_g phonons are coupled at the high fluence excitation, and, furthermore, *both* exhibit the collapse and revival of their amplitudes. Our data show that the dynamics of doubly degenerate phonons at high fluence and low temperature in many aspects replicate that of the fully symmetric phonons [8, 10], even though the two modes couple with electronic excitation in a quite different manner.

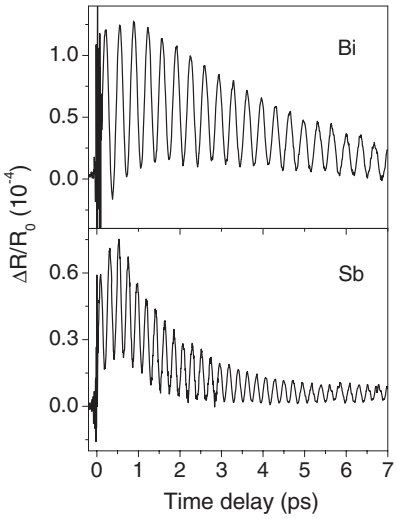

Figure 1. Normalized pump–probe data for Bi (upper panel) and Sb (lower panel) taken at room temperature and low fluence ($F = 0.02$ mJ cm^{-2}) excitation. The irregular structure around zero delay is a coherent artefact.

2. Experimental details

In this study we used the single crystals of bismuth (Bi) and antimony (Sb) with surfaces perpendicular to the trigonal axis (0001). The crystals were mounted into a closed-cycle cryostat, and the measurements were performed for different temperatures in the range of 7–300 K. Transient reflectivity measurements were performed in a degenerate pump–probe scheme, in which the amplified laser pulses having the centre wavelength of 800 nm and the durations of 140 fs were divided into the pump and probe beams. Their polarizations were perpendicular to each other with the pump polarization along the bisectrix axis of the crystals. Phase-sensitive detection was carried out by modulating the pump beam at 2 kHz with an optical chopper and the reflected probe signal detected by a p–i–n photodetector was analysed with a lock-in amplifier. In isotropic detection, the beam polarizations were perpendicular to each other with the pump polarization along the bisectrix axis of the crystals. Here we detected the reflected probe beam of the same polarization as the incident one, and the difference between the signal (with the sample) and reference (without the sample) was recorded. In anisotropic measurements, the probe beam polarized at 45° relative to the bisectrix axis was analysed into components parallel to the binary and bisectrix axis. In this case, the difference between the components was detected. Above a threshold $F_{\mathrm{th}} \approx 23$ mJ cm^{-2}, we observed permanent damage under an optical microscope, and the transient reflectivity signal was irreversibly changed for both Bi and Sb. Therefore all our measurements were made at fluence below the damage threshold F_{th}. Further details of the experimental technique can be found elsewhere [6, 8, 10, 12].

3. Experimental results

A typical normalized pump–probe signal obtained for a semimetal at room temperature and low pump fluence consists of non-oscillatory (electronic) and oscillatory (phononic) contributions,

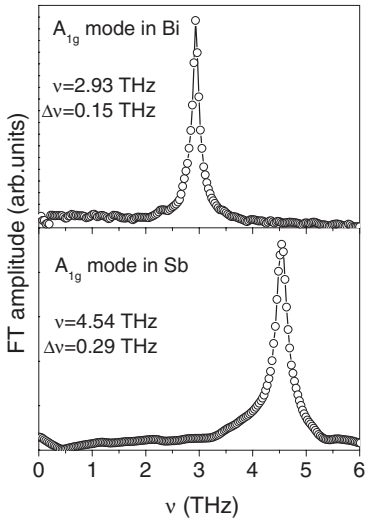

Figure 2. Fourier transforms of the oscillatory part in Bi (upper panel) and Sb (lower panel). The parameters of a Lorentzian fit are shown in each panel.

as shown in figure 1 for bismuth and antimony:

$$\frac{\Delta R}{R_0} = A_e \exp\left(-\frac{t}{t_e}\right) + A_p \exp\left(-\frac{t}{t_p}\right) \sin(2\pi \nu t + \varphi). \tag{2}$$

Here A_e and t_e are the electronic initial amplitude and decay time, A_p and t_p are the initial amplitude and decay time of the fully symmetric A_{1g} coherent phonon, ν is the phonon frequency, and φ is the initial phase. The amplitude ratio A_p/A_e depends on the material (at $\lambda = 800$ nm it is larger in bismuth than in antimony), temperature, fluence and excitation/probe wavelength.

At low fluence and room temperature, the oscillatory part of the transient reflectivity of Bi and Sb shown in figure 1 is solely due to fully symmetric phonons. Fourier transforms (FTs) of the oscillations give correspondingly a single Lorentzian peak centred at 2.93 THz in Bi and at 4.54 THz in antimony; see figure 2. At moderate fluence (>1 mJ cm^{-2}) and low temperature, the transient reflectivity is much more complicated with several different frequencies evolving in time. The transient reflectivity of Bi shown in figure 3 suggests a multilevel lattice coherence determining the ultrafast dynamics. Indeed, FTs presented in figure 4 for both (isotropic and anisotropic) detection types display a number of modes. A similar spectrum at high fluence excitation is observed for antimony; see figure 5. For a higher pump fluence, the lifetimes of coherent oscillation in both materials became shorter, and the initial frequencies experience a downshift. Analysis of the A_{1g} oscillation in antimony shows that the frequency at a relatively high fluence is time dependent with a larger phonon chirp at higher excitation level as previously observed for bismuth [5, 6, 8, 10, 12]. Increasing fluence further results in the emergence of the collapse and revival (recurrence) of the coherent amplitude; see figure 6 for bismuth. The wavelet transform of this collapsing and reviving signal shown in figure 7 reveals striking details of the spectral and temporal structures that have little in common with the low fluence case. It is first instructive to cut the three-dimensional wavelet transform along the time axis at a fixed frequency, as shown for the frequencies of A_{1g} and E_g phonons in figure 8. Such temporal slices reveal that not only the A_{1g} but also the E_g phonon exhibits collapse and revival of amplitude, in which with increasing time the amplitude decreases almost to zero at 'collapse

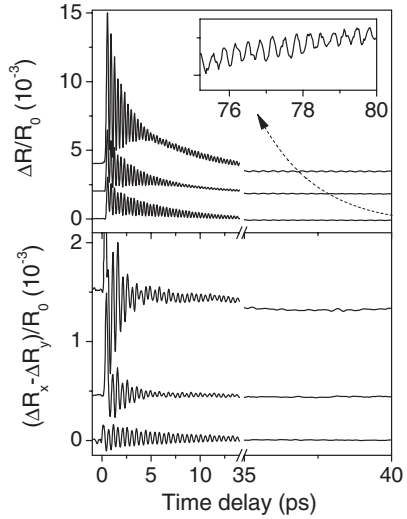

Figure 3. Normalized pump–probe data for Bi taken for different pump powers at $T = 7$ K with the isotropic (upper panel) and anisotropic detection (lower panel). The traces are offset for clarity and the fluences are 6.9, 5.4, and 1.9 mJ cm^{-2} (from top to bottom). The inset in the upper panel depicts the oscillations at longer time delays not shown in the figure for the fluence equal to 1.9 mJ cm^{-2}.

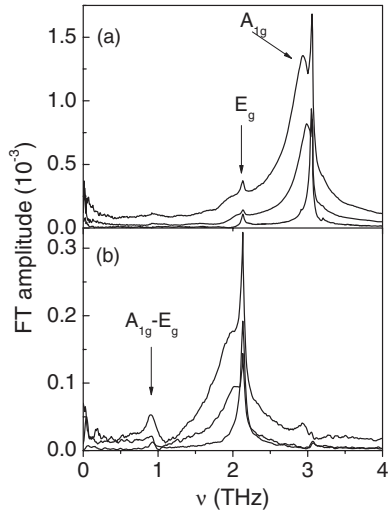

Figure 4. Fourier transforms of the oscillatory traces shown in figure 3 for the isotropic (a) and anisotropic (b) detection.

time' and then increases again reaching a maximum at 'revival time'. As easily seen from figure 8, the characteristic times of this collapse–revival are shorter for the E_g than for the A_{1g} phonon and the revival is more evident for the fully symmetric mode. In this recurrence regime, both A_{1g} and E_{1g} modes with asymmetric line shapes and their combinations are clearly seen in the FT spectrum of both bismuth and antimony; see figures 4 and 5. Thus, in semimetals at high fluence and low temperature there is a significant contribution not only from the E_g phonon, but also from the combinations of E_g and A_{1g} phonons both absent at low fluence

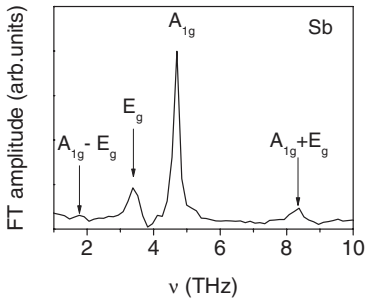

Figure 5. Fourier transform of the oscillatory trace taken at $T = 7$ K and $F = 6.5$ mJ cm^{-2} for Sb with isotropic detection.

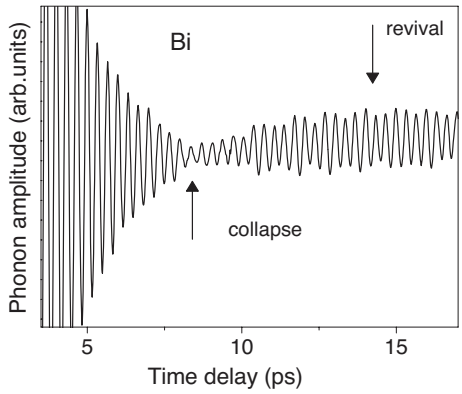

Figure 6. Coherent oscillations in bismuth (after the removal of the non-oscillating background) demonstrating collapse and revival in Bi at $T = 7$ K and $F = 9.5$ mJ cm^2.

excitation. However, it should be noted that the combination modes appear only at relatively high fluence almost simultaneously with the collapse and revival phenomenon, whereas the doubly degenerate phonons are present at any fluence provided the crystal temperature is below 200 K for antimony, or below 150 K for bismuth. The very appearance of the combination modes is indicative of a correlation between two originally uncoupled phonon modes.

For the fully symmetric mode, the Raman tensor $\frac{\partial \alpha}{\partial Q}$ for a basal plane is reduced to a scalar quantity a. As a result, the anisotropic detection, in which two polarization components $R_{\parallel}$ and $R_{\perp}$ after reflection on the [0001] surface are recorded, should cancel the contribution of A_{1g} phonon. Contrary to this expectation, the anisotropic reflectivity measurement on our bismuth crystal sometimes showed a quite strong contribution from the fully symmetric oscillations indicating the selection rule breakdown. This breakdown may stem from some form of surface disorder as it was previously observed in spontaneous Raman measurements [20] and suggests that even below the damage threshold of $F_{\rm th} \approx 23$ mJ cm^{-2}, the high fluence pulses bring in some modification of the crystal structure. However, the anisotropic detection experiments on fresh (not exposed to high fluence radiation) regions of the crystal show that the coherent oscillations are predominantly produced by doubly degenerate modes, and the Raman selection rules are strictly obeyed for both modes.

To clarify the physics behind the appearance of the E_g mode in semimetals at low temperature and high fluence, we measured both temperature and fluence dependences of the

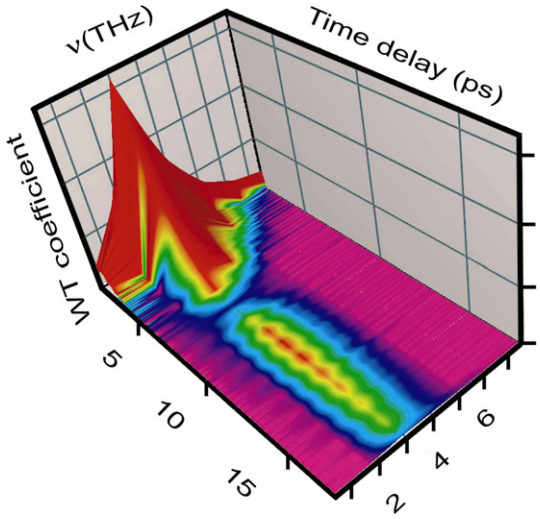

Figure 7. Wavelet transform of the collapsing and reviving oscillations shown in figure 6. (This figure is in colour only in the electronic version)

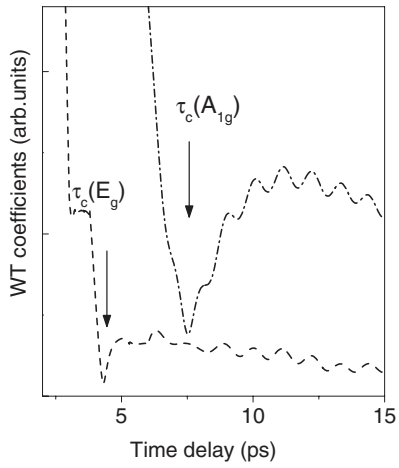

Figure 8. Time profiles of the A_{1g} and E_g phonons in Bi obtained from cross-sections of the time–frequency spectrum of figure 6 at two different frequencies of 3 and 2 THz, respectively. The amplitude modulation is an artefact of the wavelet transform related to a finite time window size.

coherent oscillations in bismuth. To obtain the temperature dependence, we fixed the pump fluence at $F = 4$ mJ cm^{-2} and traced the coherent amplitudes of A_{1g} and E_g modes obtained from the peak height in the FT spectrum, as well as the amplitude ratio $\beta = A_{1g}/E_g$ as a function of temperature. Such analysis underestimates the contribution of E_g oscillations since there is a significant line broadening of this mode at elevated temperatures. Therefore, in addition, we traced the coherent amplitudes of A_{1g} and E_g modes obtained from a fit in the time domain to a damped harmonic function (for a time span of 4 ps). In both cases shown in figures 9 and 10, a higher temperature leads to a decreased contribution from the E_g mode, which is almost negligible above 150 K. The A_{1g} amplitude in figure 9 shows a weak decrease with temperature at low temperature, followed by an abrupt decrease between 140

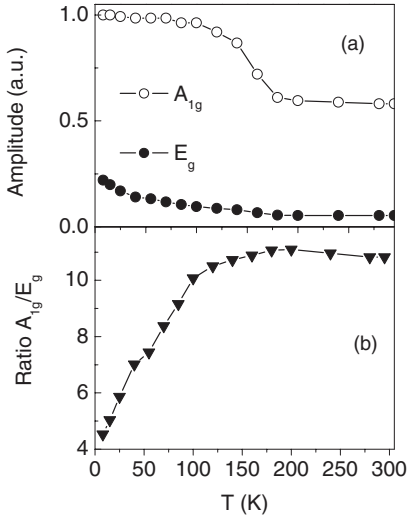

Figure 9. The FT peak heights of E_g and A_{1g} phonons in bismuth obtained from the oscillatory part of the isotropic reflectivity at $F = 4$ mJ cm^{-2} (a), and their ratio (b) as a function of temperature.

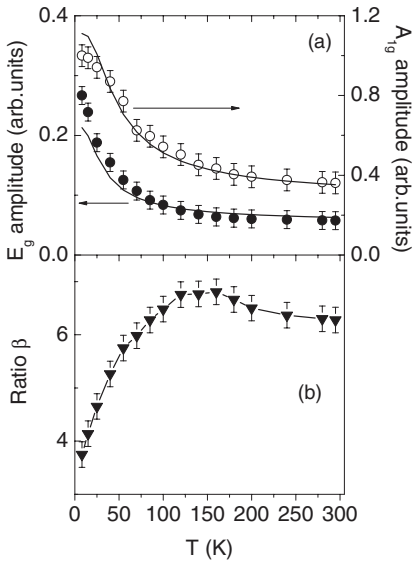

Figure 10. Coherent amplitudes of E_g and A_{1g} phonons in Bi obtained from the fit in real time of the oscillatory part of the isotropic reflectivity at $F = 4$ mJ cm^{-2} (a), and their ratio (b) as a function of temperature. In the upper panel solid lines are the fits to the Raman cross-section as described in the text.

and 190 K. These observations suggest that thermal occupation of the phonon mode inhibits the creation of lattice coherence. We fitted the temperature data in figure 10 to the expected temperature dependence of the peaked intensity of spontaneous Raman scattering assuming a Lorentzian line shape with the linewidth controlled by anharmonic decay. The Raman cross-section increases monotonically with temperature following the Bose–Einstein statistical factor

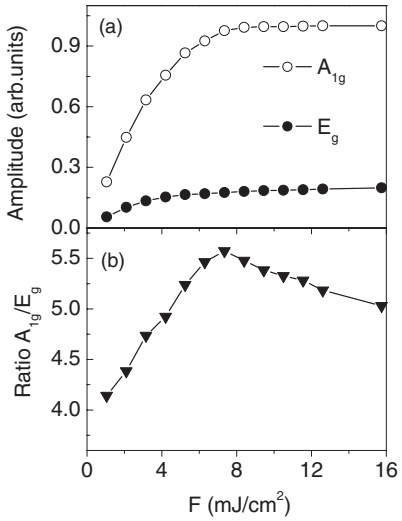

Figure 11. The FT peak heights of E_g and A_{1g} phonons in Bi obtained from the oscillatory part of the isotropic reflectivity at 7 K (a) and their ratio (b) as a function of pump fluence.

$n(\nu)+1$; therefore using the well-known property of a Lorentzian, the temperature dependence of peak intensity is proportional to $\frac{n(\nu)+1}{2n(\frac{\nu}{2})+1}$. The agreement between the experimental data and the Raman cross-section in figure 8 is qualitatively good for $T > 30$ K. For lower temperatures, the experimental points deviate significantly.

We also measured the fluence dependence in bismuth at a fixed temperature of 7 K. As the pump fluence is increased, the amplitude ratio β first grows and then slightly decreases as shown in figure 11. This is mainly because at high fluence the A_{1g} amplitude saturates faster than the E_g amplitude. The frequencies and lifetimes of both modes gradually decrease with pump fluence. In addition, we observe a strong similarity of the overall line shapes of the two modes: the line shape for the E_g phonon replicates that for the A_{1g} phonon at any fluence. In the high fluence regime, FTs of the oscillations show minor sharp peaks that appear on the high energy side of the main broad peaks for each phonon mode; see figure 4. The frequency of the sharp peak produced by the long-lived component in the time domain is almost independent of the fluence, coinciding with that observed at low fluence for each mode. This doublet structure shown in figure 4 might be simply due to oscillations in the presence (broad feature) and absence (narrow feature) of photoexcited carriers. However, as will be shown below, the line shape of the broad feature demonstrates a cyclic behaviour not compatible with the irreversible decay of the carrier density.

A further interesting aspect is related to the initial phase of the A_{1g} and E_g phonons. To determine the initial phase more precisely, we fit the oscillatory transient obtained with $F = 0.5$ mJ cm^{-2} (the relatively low fluence is needed to avoid the complication of chirped character of the oscillation) to

$$A_A \exp(-t/\tau_A)\sin(2\pi\nu_A+\phi) + A_E \exp(-t/\tau_E)\sin(2\pi\nu_E+\varphi). \tag{3}$$

The results of the fit using (3) clearly indicate that the generation of the coherent phonon is essentially displacive for the A_{1g} phonon (a cosine behaviour) and mainly impulsive for the E_g phonons (a sine behaviour); see figure 12. Even though uncertainty in the determination of time zero does not allow us to ascribe pure cosine or sine behaviour for the modes, the relative phase

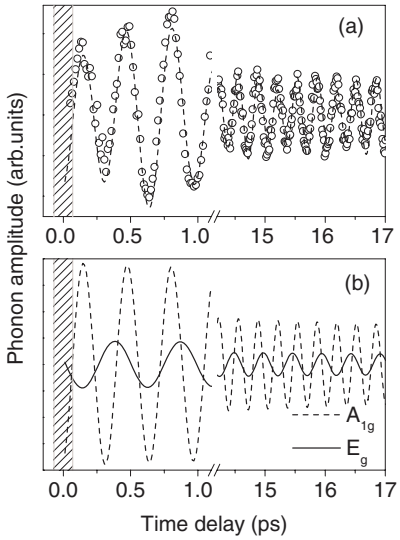

Figure 12. (a) Coherent oscillations in Bi. The oscillations were obtained in isotropic detection with $F = 0.45$ mJ cm^{-2} at 7 K after the removal of the non-oscillating background. The open symbols and the dashed curve represent the experimental points and the fit with equation (3), respectively. (b) Two components of the fit in (a), indicating the displacive excitation with an initial phase of $-\pi/2$ for the A_{1g} phonon (solid curve) and the impulsive excitation with an initial phase of $-\pi$ for the E_g phonon (dashed curve).

defined with a higher accuracy is very close to $\pi/2$. Indeed, if we assign an error to the phase equal to the acquisition step of the time delay multiplied by the phonon frequency [22], then in our experiments an error of 13 fs in the delay gives a 15° error in the A_{1g} phase and a 10° error in the E_g phase. Such systematic errors cannot explain the $\pi/2$ gap in figure 12 between the phases of the two modes.

A cut of the wavelet transform shown in figure 7 along the frequency axis allows inspecting the time dependence of a chosen frequency. A time windowed FT, the results of which are presented in figure 13, gives us almost equivalent information with a higher frequency resolution. One can easily see that the spectral content of the transient signal in the high fluence regime is a function of time. As the time window shifts in time by a 75 fs step, the line shapes of phonons change drastically. Indeed, the line shape of the E_g mode is strongly asymmetric and sometimes resembles a dispersion-like curve. More exactly, the E_g peak first disappears (it is rather a dip than a peak), then reappears at higher frequency, and finally moves to lower frequency. Similar cyclic temporal behaviour is also observed for the difference mode ($A_{1g} - E_g$). For the A_g phonon, the spectral profiles vary from a single broad peak with a hole bored approximately at the centre, to dispersive profiles, and then to a simply asymmetric peak for longer time delays.

Concluding the experimental section it will be appropriate to summarize the observed similarities of and differences between the A_{1g} and E_g phonons excited by high fluence pulses at low temperature:

- both modes experience downshift in frequency and become significantly broader at higher fluence;
- both modes follow the selection rules prescribed by Raman scattering and their temperature dependences roughly coincide with that of a Raman cross-section;

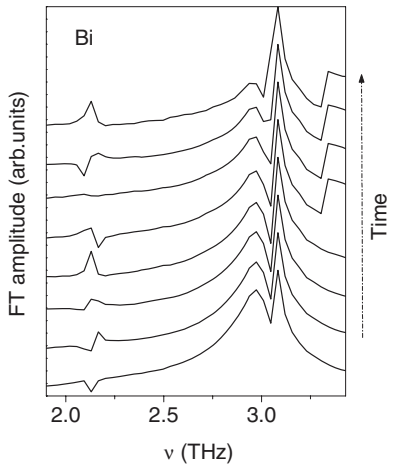

Figure 13. Time window dependence of the FT spectrum of the oscillatory part of the isotropic reflectivity of Bi at 7 K at 8.5 mJ cm^{-2}. Each consecutive spectrum was obtained for 15 ps wide time windows including the collapse–revival, by shifting the window by 75 fs from the one below (bottom: 5–15 ps, top: 5.45–15.45 ps).

- both modes demonstrate time-dependent spectra;
- both modes exhibit the collapse and revival above approximately the same threshold fluence, but with different characteristic times;
- the initial phases for the E_g and A_{1g} modes are $\pi/2$ shifted;
- at high excitation the two modes are coupled.

4. Discussion

In order to understand differences and similarities in the behaviour of A_{1g} and E_g symmetry phonons, we have first to identify their generation mechanism. In the displacive model, the *instantaneous* electronic excitation leads to a sudden change in the free energy of the crystal lattice, which responds to the new excited electronic state by moving toward a new equilibrium position. In this model, lattice coherence is created in an excited electronic state, and the inertia of the lattice causes atoms to oscillate around the new equilibrium in a cosine fashion. Conversely, purely impulsive excitation leads to a strict sine motion indicating oscillations around non-shifted atomic equilibrium positions with the coherence created in the ground electronic state. Therefore, the initial phase of the phonon oscillation can serve as the means to identify the generation mechanism [1, 17]. According to the observed $\pi/2$ shift we can state that the fully symmetric mode is excited predominantly displacively with the lattice coherence created in an excited electronic state, whereas the doubly degenerate mode is primarily generated impulsively with the coherence in the ground electronic state. In this explanation, the $\pi/2$ shifted initial phases for different symmetry phonons are simply a result of the coupling to virtual and real charge-density fluctuations for E_g and A_{1g} modes, respectively. By coupling to a virtual intermediate state, ultrashort light pulses give an impulsive force because of the very short fluctuation lifetime. In contrast, a real transition shifts the equilibrium position of the lattice atoms with a typical lifetime comparable to that of the Raman coherence.

Next we consider the question of why the doubly degenerate phonons are effectively excited only at low temperature or high fluence. The answer is most likely related to the

fact that the pump–probe experiment is influenced by the modulation of quantum fluctuations since the experiment probes $\langle Q \rangle$. At elevated temperature, the thermal population of the E_g phonons which is larger than that of the A_{1g} phonons hinders the creation of coherence (to put it differently, the coherent amplitude $\langle Q \rangle$ for E_g phonons is smaller than the square root of the corresponding atomic mean square displacement $\sqrt{\langle \Delta u^2 \rangle}$). Only at low enough temperature, which controls the population, or at high enough excitation level, which is responsible for the coherent amplitude $\langle Q \rangle$, can one attain the condition $\langle Q \rangle > \sqrt{\langle \Delta u^2 \rangle}$ necessary for the coherent phonon detection.

Now we focus on the processes responsible for the appearance of combination modes and asymmetric phonon line shapes in the FT spectra. To describe the emergence of the combination modes it will be enough to consider either a direct coupling between the phonons of different symmetries arising due to third- and fourth-order anharmonic coupling, or to bring about an indirect mode–mode coupling, possibly via electronic excitations. The anharmonic coupling will result, apart from a shift and broadening of the modes, in the emergence of additional frequencies arising through accidental degeneracy of highly excited phonon states and leading to beats of a type called accidental quantum beats [23]. The indirect coupling corresponds to the next order in the hierarchy of possible interactions and takes into account electron–phonon coupling. This sort of coupling (which seems to be more realistic one) will automatically result in asymmetric line shapes and be controlled by a strength (density of states) of continuum that is fluence dependent. An asymmetric spectral shape is usually formed [24] if a transition from a given state $|a\rangle$ into a state $|b\rangle$ is energetically degenerate with transitions from $|a\rangle$ into a continuum of states $|E_i\rangle$, provided that the state $|b\rangle$ is coupled to the continuum $|E_i\rangle$. However, our attempts to fit the experimental E_g line shapes with the Fano formula

$$V = \frac{(\varepsilon + q)^2}{1 + \varepsilon^2} \tag{4}$$

with a dimensionless energy ε of the discrete transition in units of its decay and an asymmetry parameter q revealed that q changes its sign as a function of time. Such unusual behaviour indicating the violation of time-reversal symmetry was discussed in detail in [12].

Finally, we briefly address the collapse and revival at the frequencies of fully symmetric and doubly degenerate phonons. The revival is a universal feature of the long time behaviour of weakly anharmonic oscillators occurring if the spectrum is nearly quadratic, and if the fundamental frequency is significantly larger than the anharmonicity [25]. In this regime the short time behaviour of the mode is harmonic: it oscillates back and forth, while anharmonic effects govern the long time evolution. Such a regime is indeed realized for A_{1g} phonons [6, 8, 10], but most likely not for E_g ones. In fact, there are only several E_g cycles occurring before the collapse sets in; thus one can hardly consider the short time behaviour for the E_g mode as harmonic. The revival time is proportional to the lattice anharmonicity through the $\frac{\partial \nu}{\partial E}$ term in which ν is the classical frequency, E is the oscillator energy [25]. Therefore, an almost twice shorter revival time for the E_g mode might imply that the anharmonicity of its potential is four times larger than that for the A_{1g} mode. However, the larger E_g anharmonicity is not supported by the E_g chirp magnitude, which is smaller than that of the A_{1g} phonon. It may happen that the phenomenon for the E_g mode can be somewhat different. For the A_{1g} mode, the origin of the recurrence is the anharmonicity within a single phonon mode. In contrast, the collapse and revival of the E_g mode can emerge from the coupling between the A_{1g} and E_g degrees of freedom. Therefore, for doubly degenerate phonons, the revival time is controlled not by the anharmonicity of its potential but rather by the coupling (either

anharmonic or indirect) between the two modes. In some sense, the situation with the E_g phonon may be similar to that occurring in diatomic molecules where resonant driving of certain electronic transitions yields collapses and revivals of the electronic populations due to the quantized vibrational motion of the nuclei [26].

5. Conclusion

In summary, we have performed a comprehensive investigation of the coherent phonons of different symmetry in bismuth and antimony under various temperature and excitation conditions. Three observations are important. (i) With decreasing temperature we can increase the number of phonon modes observed in the time domain since at low temperature and any excitation level, both A_{1g} and E_g coherent phonons appear in the time-resolved reflectivity. The fact that E_g coherent phonons disappear at room temperature, whereas A_{1g} phonons do not, can be explained by a smaller thermal population of the latter mode. (ii) The relative initial phase of the A_{1g} and E_g oscillations in bismuth testifies that the fully symmetric mode is excited for the most part displacively, whereas the doubly degenerate mode is driven impulsively. This result suggests that the A_{1g} phonon couples to a real charge-density fluctuation, whereas the E_g phonon couples to a virtual one. (iii) At high excitation level, the two modes are coupled and furthermore behave in a similar way: an initial fast decay of oscillations is followed by weak recurrence with much slower decay, but the characteristic times of the recurrence are shorter for the doubly degenerate phonons.

Acknowledgments

This work was supported through the joint grant 05-02-19910 by the Russian Foundation for Basic Research and the Japan Society for Promotion of Science, the grants 04-02-97204-p and 06-02-16186-a from the Russian Foundation for Basic Research, and KAKENHI-17540305 and 18340093.

References

[1] Merlin R 1997 *Solid State Commun.* **102** 207
[2] Dekorsy T, Cho G C and Kurz H 2000 *Light Scattering in Solids VIII* ed M Cardona and G Güntherodt (Berlin: Springer) p 169
[3] Hunsche S, Wienecke K, Dekorsy T and Kurz H 1995 *Phys. Rev. Lett.* **75** 1815
[4] DeCamp M F, Reis D A, Bucksbaum P H and Merlin R 2001 *Phys. Rev.* B **64** 092301
[5] Hase M, Kitajima M, Nakashima S and Mizoguchi K 2002 *Phys. Rev. Lett.* **88** 067401
[6] Misochko O V, Hase M and Kitajima M 2003 *JETP Lett.* **78** 75
[7] Sokolowski-Tinten K, Blome C, Blums J, Cavalleri A, Dietrich C, Tarasevitch A, Uschmann I, Förster E, Kammler M, Horn-von-Hoegen M and von der Linde D 2003 *Nature* **422** 287
[8] Misochko O V, Hase M, Ishioka K and Kitajima M 2004 *Phys. Rev. Lett.* **92** 197401
[9] Roeser C A D, Kandyla M, Mendioroz A and Mazur E 2004 *Phys. Rev.* B **70** 212302
[10] Misochko O V, Hase M, Ishioka K and Kitajima M 2004 *Phys. Lett.* A **321** 381
[11] Murray É D, Fritz D M, Wahlstrand J K, Fahy S and Reis D A 2005 *Phys. Rev.* B **72** 060301(R)
[12] Misochko O V, Hase M, Ishioka K and Kitajima M 2005 *JETP Lett.* **82** 426
[13] Cheng T K, Brorson S D, Kazeroonian A S, Moodera J S, Dresselhaus G, Dresselhaus M S and Ippen E P 1990 *Appl. Phys. Lett.* **57** 1004
[14] Cheng T K, Acioli L H, Vidal J, Zeiger H J, Dresselhaus G, Dresselhaus M S and Ippen E P 1993 *Appl. Phys. Lett.* **62** 1901
[15] Zeiger H J, Vidal J, Cheng T K, Ippen E P, Dresselhaus G and Dresselhaus M S 1992 *Phys. Rev.* B **45** 768
[16] Hase M, Mizoguchi K, Harima H, Tani M, Sakai K and Hangyo M 1996 *Appl. Phys. Lett.* **69** 2474
[17] Lobad A I and Taylor A J 2001 *Phys. Rev.* B **64** 180301

[18] Stevens T E, Kuhl J and Merlin R 2002 *Phys. Rev.* B **65** 144304
[19] Lannin J S, Calleja J M and Cardona M 1975 *Phys. Rev.* B **12** 585
[20] Bansal L and Roy A P 1985 *Phys. Rev.* B **33** 1526
[21] Dekorsy T, Auer H, Bakker H J, Waschke C, Roskos H G, Kurz H, Wagner W and Grosse P 1995 *Phys. Rev. Lett.* **74** 738
[22] Bragas A V, Aku-Leh C, Costantino S, Ingale A, Zhao J and Merlin R 2004 *Phys. Rev.* B **69** 205306
[23] Merchant K A, Thompson D E and Fayer M D 2002 *Phys. Rev.* A **65** 023817
[24] Fano U 1961 *Phys. Rev.* **124** 1866
[25] Averbukh I Sh and Perelman N F 1989 *Phys. Lett.* A **139** 449
[26] Domokos P, Kiss T, Janszky J, Zucchetti A, Kis Z and Vogel W 2000 *Chem. Phys. Lett.* **322** 255